Effect of bending and torsional mode excitation on the reaction $Cl+CH_4 \rightarrow HCl+CH_3$

Zee Hwan Kim,[a] Hans A. Bechtel, Jon P. Camden, and Richard N. Zare[b]
Department of Chemistry, Stanford University, California 94305-5080

(Received 8 September 2004; accepted 9 November 2004; published online 15 February 2005)

A beam containing CH_4, Cl_2, and He is expanded into a vacuum chamber where CH_4 is prepared via infrared excitation in a combination band consisting of one quantum of excitation each in the bending and torsional modes ($\nu_2+\nu_4$). The reaction is initiated by fast Cl atoms generated by photolysis of Cl_2 at 355 nm, and the resulting CH_3 and HCl products are detected in a state-specific manner using resonance-enhanced multiphoton ionization (REMPI). By comparing the relative amplitudes of the action spectra of $Cl+CH_4(\nu_2+\nu_4)$ and $Cl+CH_4(\nu_3)$ reactions, we determine that the $\nu_2+\nu_4$ mode-driven reaction is at least 15% as reactive as the ν_3 (antisymmetric stretch) mode-driven reaction. The REMPI spectrum of the CH_3 products shows no propensity toward the formation of umbrella bend mode excited methyl radical, $CH_3(\nu_2=1)$, which is in sharp distinction to the theoretical expectation based on adiabatic correlations between CH_4 and CH_3. The rotational distribution of $HCl(v=1)$ products from the $Cl+CH_4(\nu_2+\nu_4)$ reaction is hotter than the corresponding distribution from the $Cl+CH_4(\nu_3)$ reaction, even though the total energies of the two reactions are the same within 4%. An explanation for this enhanced rotational excitation of the HCl product from the $Cl+CH_4(\nu_2+\nu_4)$ reaction is offered in terms of the projection of the bending motion of the CH_4 reagent onto the rotational motion of the HCl product. The angular distributions of the $HCl(\nu=0)$ products from the $Cl+CH_4(\nu_2+\nu_4)$ reaction are backward scattered, which is in qualitative agreement with theoretical calculation. Overall, nonadiabatic product vibrational correlation and mode specificity of the reaction indicate that either the bending mode or the torsional mode or both modes are strongly coupled to the reaction coordinate. © *2005 American Institute of Physics*. [DOI: 10.1063/1.1844295]

I. INTRODUCTION

In contrast to stretch-activated reactions,[1–6] the effects of bending (we shall refer to all nonstretching modes as bending modes for simplicity in what follows) excitation on atom+polyatom reactions have been largely unexplored, and only a few, indirect experimental reports exist to date.[7–9] For example, Bronikowsi, Simpson, and Zare[9] observed minor effects of the bending vibration in the reaction $H+D_2O \rightarrow HD+OD$, whereas Woods, Cheatum, and Crim found *decreased* reactivity of Cl+HNCO upon bending-mode excitation. Because the bending vibrations involve concerted motion of three or more atoms in a polyatomic molecule, correct theoretical modeling of the bending-mediated reactions requires a description of the polyatomic reagent beyond the simple, isolated reactive bond picture, and this fact imposes theoretical and computational challenges.[10,11] Currently, there is no generally accepted view concerning the effects of bending vibrational excitation on bimolecular reactions, partly owing to the scarcity of experimental examples.

The enhanced reactivity of low-frequency bending-mode excited methane on the $Cl+CH_4$ reaction has been implicated by several experimental and theoretical studies. Corchado, Truhlar, and Espinosa-Garcia[12] and Yu and Nyman[13,14] showed that the ν_4 (bending) mode of methane adiabatically correlates to the ν_2 (out-of-plane umbrella bending) mode of the methyl radical product, and that this vibrational adiabat is closely coupled to the reaction coordinate. Therefore, they predicted that ν_4 excitation of methane should enhance its reactivity and produces more umbrella bending excited $CH_3(\nu_2)$ products. Quantum scattering calculations on the $Cl+CH_4(2\nu_4)$ reaction by Skokov and Bowman[15] predict a bimodal rotational distribution of the HCl products that directly reflects the initial bending vibration of the methane reagent. Experimentally, Kandel and Zare[16] measured the speed distributions and the spatial anisotropies of the methyl radical products from the reaction of $Cl+CH_4(\nu=0)$, and found abnormally fast-moving methyl radical products. These abnormal speed distributions and the spatial anisotropy were explained by the enhanced reactivity of the residual ν_2- or ν_4-mode excited methane present in the supersonic expansion. Furthermore, they also proposed that the ν_2- or ν_4-mode enhancement could explain non-Arrhenius behavior observed in low-temperature kinetics measurement of $Cl+CH_4$ reaction.[17] Recently, Zhou *et al.*[18] reexamined the role of the spin–orbit-excited chlorine atom $[Cl^*(^2P_{1/2})]$ and excitation of the ν_2- or ν_4-mode excitation in the $Cl+CH_4$ reaction. They found only a modest reactivity enhancement associated with ν_2- or ν_4-mode excitation. To

[a]Present address: Department of Chemistry, University of California, Berkeley, California 94720.
[b]Author to whom correspondence should be addressed. Electronic mail: zare@stanford.edu

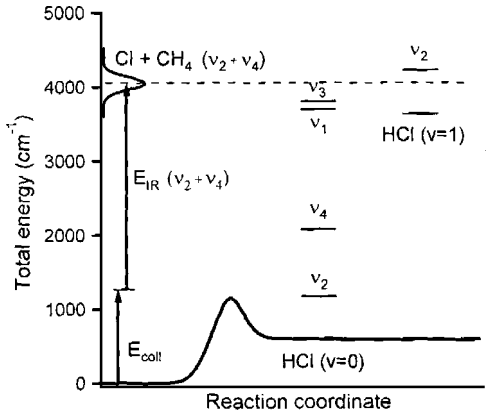

FIG. 1. Schematic energetics of the reaction $Cl+CH_4(\nu_2+\nu_4)\rightarrow HCl+CH_3$. The collision energy spread is represented by a Gaussian distribution estimated using the formulas of van der Zande *et al.* (Ref. 27) at 15 K. The $\nu_2+\nu_4$ mode (2855 cm^{-1}) excited methane is prepared by direct infrared pumping. Also shown on the right side of the reaction coordiate are the fundamental frequencies of the CH_3 normal modes superimposed on top of the vibrational levels of the HCl.

date, it seems fair to state that the importance of ν_2- or ν_4-mode excitation in the $Cl+CH_4$ reaction is not completely understood.

In this work, we examine the effects of torsional ν_2 and bending ν_4 mode excitations on the reaction,

$$Cl + CH_4(\nu_2 + \nu_4) \rightarrow HCl + CH_3, \quad (1)$$

in which the methane is prepared in the $\nu_2+\nu_4$ combination band by IR excitation. The photoloc technique[2] is used to obtain state-resolved differential cross sections (DCSs) of the products. Because the ν_2 transition is IR-inactive and intense IR radiation required for the direct excitation of ν_4 (1306 cm^{-1}) is not readily available, excitation of the $\nu_2+\nu_4$ combination band of methane offers a convenient route to the investigation of the effects of bending and torsional mode excitation on the $Cl+CH_4$ reaction. Because the energy of the $\nu_2+\nu_4$ mode (2855 cm^{-1}) is nearly the same as that of antisymmetric stretch ν_3 mode (3019 cm^{-1}), this reaction also provides an excellent opportunity to compare the outcome of two different, yet nearly isoenergetic vibrational excitations of methane as well. Therefore, we have made an extensive comparison of the dynamics for the reaction of Cl atoms with $CH_4(\nu_3)$ and with $CH_4(\nu_2+\nu_4)$.

II. ENERGETICS AND EXPERIMENTAL PROCEDURES

Figure 1 displays the relevant energetics for the $Cl+CH_4\rightarrow HCl+CH_3$ reaction. The reaction is slightly endothermic ($\Delta H^0=660$ cm^{-1}), and the estimated[19] reaction barrier is $\sim$1000 cm^{-1}. Photodissociation of Cl_2 at 355 nm provides 1290 ± 100 cm^{-1} of center-of-mass (CM) collision energy E_{coll}, and the $\nu_2+\nu_4$ mode vibrational excitation provides 2855 cm^{-1} extra energy, giving a total available energy of 4145 cm^{-1}, which is above the reaction barrier. Also shown in Fig. 1 are the energetically accessible vibrational energy levels of HCl and CH_3 (ν_1, symmetric stretching, 3004 cm^{-1}; ν_2, umbrella bending, 610 cm^{-1}; ν_3, antisymmetric stretching, 3161 cm^{-1}; ν_4, deformation, 1400 cm^{-1}) products. Vibrationally excited CH_3 products can be formed coincidentally with the HCl($v=0$) products, but only the vibrationally ground-state CH_3 products are allowed to form with HCl($v=1$) products.

The methods and experimental apparatus have been described in detail previously,[2] and only the essential features are presented here. A 1:4:5 mixture of molecular chlorine (Matheson, research grade, 99.999%), methane (Matheson, research purity, 99.999%), and helium (Liquid Carbonic, 99.995%) gases is supersonically expanded into the extraction region of a linear Wiley-McLaren time-of-flight (TOF) spectrometer under single-collision conditions. Photodissociation of Cl_2 with linearly polarized 355 nm light produces fast (1.6 km/s) ground-state Cl($^2P_{3/2}$) atoms via the $C\ ^1\Pi(1_u)$-$X\ ^1\Sigma(0_g^+)$ transition with a spatial anisotropy, $\beta_{phot}=-1$.[20] Methane is excited to the $\nu_2+\nu_4$ state[21,22] near 2855 cm^{-1}. After a 60–100 ns time delay for the reaction to occur, the HCl or CH_3 products are state selectively ionized by 2+1 resonance-enhanced multiphoton ionization (REMPI). The resulting ions subsequently drift along the TOF tube and are detected by Chevron-type microchannel plates. The reactive signal from the vibrationally excited methane is distinguished from background (such as HCl impurity and reactive signal from the ground-state methane) by subtracting the signal with and without IR excitation on an every-other-shot basis.

The linearly polarized 355 nm photolysis beam is generated by frequency tripling the fundamental of the output from a Nd: YAG laser (PL9020, Continuum). The IR radiation at 3.5 μm is obtained by parametrically amplifying (in a $LiNbO_3$ crystal) 3.5 μm radiation generated by difference-frequency mixing of 1.06 μm radiation (Nd: YAG fundamental output, injection seeded) and the output of a dye laser (ND6000, Continuum; LDS821, Exciton) in another $LiNbO_3$ crystal. The light for the probe REMPI process is generated by frequency doubling (in a BBO crystal) the output of a dye laser (FL2002, Lambda Physik) pumped by a Nd:YAG laser (DCR-2A, Spectra Physics). For HCl detection, we use exciton LDS489; for CH_3 detection, we use an exciton DCM/LD698 mix. The photolysis, IR, and probe beams are focused and spatially overlapped with the supersonic expansion using focal length=50 cm lenses.

The rotational distributions of the HCl products are obtained by a method similar to that of Simpson *et al.*[2] The methyl radical products are detected via the $3p_z\ ^2A''_2-X\ ^2A''_2$ transition.[23] A photoelastic modulator (PEM-80, Hinds International Inc.) flips the linear polarization direction of the photolysis laser between parallel and perpendicular to the TOF axis on an every-other-shot basis. The isotropic $\mathbf{I}_{iso}=\mathbf{I}_{\parallel}+2\mathbf{I}_{\perp}$ and anisotropic $\mathbf{I}_{aniso}=2(\mathbf{I}_{\parallel}-\mathbf{I}_{\perp})$ components of the TOF profiles are used to extract the speed-dependent spatial anisotropy of the products $\beta_{prod}(v)$, and the state-resolved DCSs by fitting these components to basis functions generated by a Monte Carlo simulation.

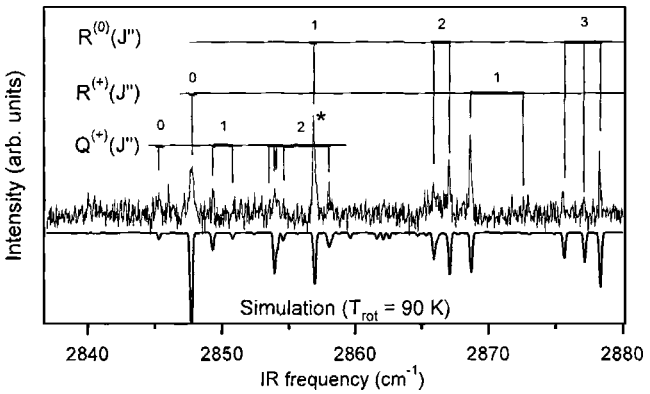

FIG. 2. Action spectrum of the reaction $Cl+CH_4(\nu_2+\nu_4) \rightarrow HCl+CH_3$, monitoring $CH_3(\nu_2)$ via the $2+1$ $^3p_{-z}$-X REMPI transition. A simulation based on HITRAN spectrum database (Ref. 21), and the assignment of transitions (Ref. 22) are also shown. The star (*) indicates the transition used in later parts of the work.

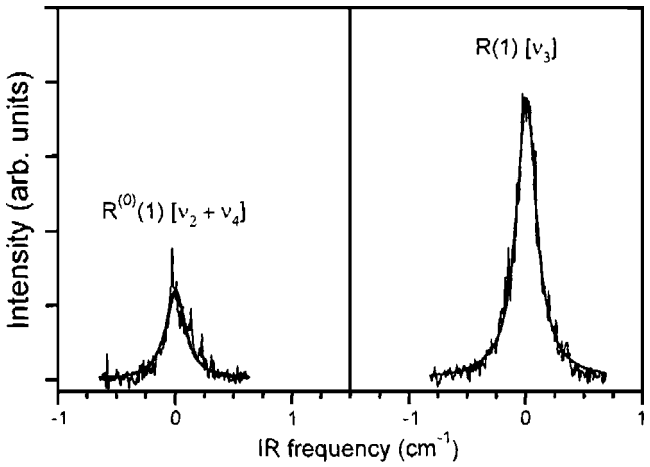

FIG. 3. Comparison of the action spectra of $R^{(0)}(1)[\nu_2+\nu_4]$ and $R(1)[\nu_3]$ transitions monitoring $CH_3(\nu_2=1)$ products. Also shown in thick solid lines are the results of fits to Lorentzian curves. The x axis is arbitrarily shifted for easy comparison of the two spectra.

III. RESULTS AND DISCUSSION

A. Reactivity enhancement upon $\nu_2+\nu_4$ mode excitation of methane

Figure 2 shows the action spectrum near the R branch of the $\nu_2+\nu_4$ band, obtained by subtracting the CH_3^+ ion signal produced on the $2+1$ REMPI 2_1^1 band without IR excitation from the signal with IR excitation. The simulated IR absorption spectrum of the $\nu_2+\nu_4$ combination band[21,22] and partial assignment of the transitions are also shown for comparison. The IR spectrum of the $\nu_2+\nu_4$ band is complicated by the interplay of the Coriolis-coupling and anharmonic perturbations.[22] In particular, Coriolis-coupling causes splitting of single rotational lines in the R branch to $R^{(+)}$, $R^{(0)}$, and $R^{(-)}$ sub-branches, depending on the coupling of rotational J and vibrational l_4 angular momenta. Anharmonic coupling further removes the degeneracy. The *positive* (enhancement) action spectrum faithfully follows the IR absorption spectrum, which unambiguously shows the *enhanced reactivity* caused by the $\nu_2+\nu_4$ mode excitation. Similar action spectra are also obtained by monitoring the $CH_3(v=0)$ or HCl products (not shown).

A quantitative comparison of the relative reactivity enhancement by exciting the ν_3 and $\nu_2+\nu_4$ modes is not straightforward because of the large difference in absorption cross sections between the two IR transitions (the $\nu_2+\nu_4$ band absorption cross section is only $\sim$5% of the ν_3 band cross section). With maximum fluence of our IR radiation, the ν_3 transition is heavily saturated, whereas the $\nu_2+\nu_4$ transition is not saturated. Therefore, we are only able to set a lower bound for the relative reaction cross sections of the $\nu_2+\nu_4$ and ν_3 mode-driven reactions, at this point. Figure 3 compares the action spectra of unsaturated $R^{(0)}(1)[\nu_2+\nu_4]$ and heavily saturated $R(1)[\nu_3]$ transitions, obtained by monitoring $CH_3(\nu_2=1)$ products. Similar spectra are also obtained by monitoring $CH_3(v=0)$ products (not shown). Because of the significantly different degrees of power broadening of the two transitions, a comparison of the integrated areas of the lines is not appropriate. Therefore, we evaluate the amplitudes of the Lorentzian[24] (saturation and power-broadened) fits of the $R^{(0)}(1)[\nu_2+\nu_4]$ and $R(1)[\nu_3]$ transitions (monitoring $CH_3(v=0)$ and $CH_3(\nu_2=1)$ products), and this analysis provides the amplitude ratio of $R^{(0)}(1)[\nu_2+\nu_4]:R(1)[\nu_3] = 0.29\pm0.14:1$ (the uncertainty of the ratio represents one standard deviation calculated from the three action spectra). From this ratio, we determine that the $\nu_2+\nu_4$ mode-driven reaction is at least 15% (with 95% statistical confidence) as reactive as the ν_3 mode-driven reaction. One might argue that the observed reactivity enhancement may originate from the residual stretching mode character present in the eigenstate of $\nu_2+\nu_4$ mode caused by a Fermi resonance. However, the stretching character in $\nu_2+\nu_4$ mode is estimated to be only 2%,[25] and as we will show later on, the rotational distributions of the $HCl(v=1)$ products are markedly different from the distributions from $Cl+CH_4(\nu_3)$ reaction. Therefore, we believe that observed reactivity enhancement is caused by the bending motion of the methane, not by the residual stretching character of the eigenstate of $\nu_2+\nu_4$. Yoon *et al.*[5] estimated the relative reactivities of the ν_1 (symmetric stretch) versus the ν_3 (antisymmetric stretch) mode of methane in the $Cl+CH_4$ reactions by comparing the action spectra of $\nu_1+\nu_4$ and $\nu_3+\nu_4$ modes. Their estimate is based on the assumption that the reactivity of the ν_4 mode character in the stretch-bend combination mode eigenstates is negligible. Our result suggests that this assumption may not be valid.

Our result is a direct experimental example of the reactive enhancement associated with the bending-mode excitation of a polyatomic reagent. Currently, we are unable to determine which mode in the $\nu_2+\nu_4$ eigenstate is mostly responsible for the observed reactivity enhancement. In a one-dimensional local-mode picture of the CH_4 bending vibration, the ν_2 and ν_4 modes appear equivalent. Theoretical calculations taking into account the full symmetry of the collision predict a marked reactivity enhancement associated with ν_4 mode excitation of the CH_4,[12–14] originating from the strong coupling of the $Cl+CH_4(\nu_4)$ adiabat to the reaction coordinate. Further experimental investigations are needed to determine the relative importance of the ν_2 and ν_4 modes in enhancing reactivity.

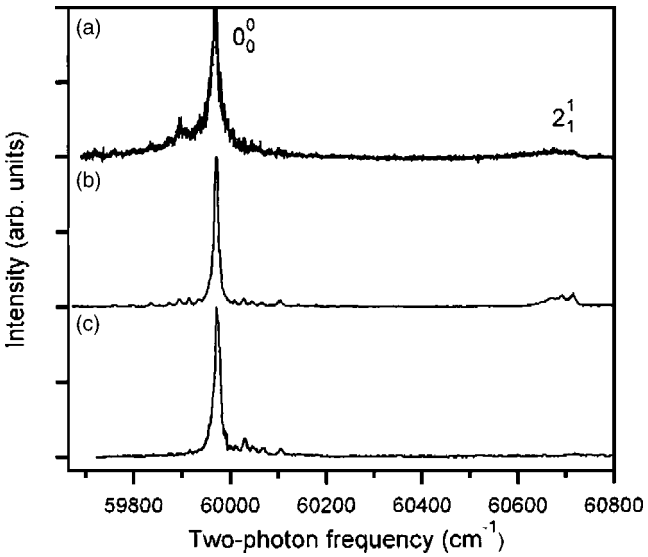

FIG. 4. $3p_z$-X 2+1 REMPI spectra of the methyl radical products from the reactions (a) $Cl+CH_4(\nu_2+\nu_4)$, (b) $Cl+CH_4(\nu_3)$, and (c) $Cl+CH_4(v=0)$.

B. Methyl radical vibrational state distributions

Figure 4 compares the 2+1 REMPI spectra of the CH_3 products from the reactions of Cl atoms with $CH_4(\nu_2+\nu_4)$, $CH_4(\nu_3)$, and $CH_4(v=0)$, covering the 0_0^0 and 2_1^1 (out-of-plane umbrella bending) bands, where we exclusively use the $R^{(0)}(1)[\nu_2+\nu_4]$ transition for the $\nu_2+\nu_4$ mode excitation of methane. All spectra have an intense 0_0^0 band, indicating that most of the CH_3 products are formed in the vibrationally ground state, regardless of the initial vibrational state. The spectra of the CH_3 products from the $Cl+CH_4(\nu_2+\nu_4)$ and the $Cl+CH_4(\nu_3)$ reactions show noticeable intensity in the 2_1^1 band, whereas the $Cl+CH_4(v=0)$ reaction produces only a negligible intensity in the 2_1^1 band. Although it is not feasible to extract the quantitative vibrational state distribution from a given REMPI spectrum of the CH_3 product because of unknown Franck–Condon factors and significant predissociation of the $3p_z\ ^2A''_2$ state used for the 2+1 REMPI probe, we calculate the ratio of the integrated intensities, $I(2_1^1)/I(0_0^0)$, of the 0_0^0 and 2_1^1 bands of CH_3 REMPI spectrum. The reactions $Cl+CH_4(\nu_2+\nu_4)$, $Cl+CH_4(\nu_3)$, and $Cl+CH_4(v=0)$ give the integrated intensity ratios of 0.21, 0.28, and 0.04, respectively (see Table I).

The ν_4 mode vibration of CH_4 adiabatically correlates to the ν_2 (umbrella bending) mode of the CH_3 product.[12] Therefore, if we assume that the ν_4 mode character is preserved in the $\nu_2+\nu_4$ eigenstate of CH_4, we expect preferential product branching into $CH_3(\nu_2=1)$ upon $\nu_2+\nu_4$ mode activation of the CH_4. Likewise, we do not expect to observe any $CH_3(\nu_2=1)$ product upon excitation of the ν_3 mode in the reaction. Our results, however, indicate no appreciable correlation between the CH_4 and CH_3 vibrations. Instead, we observe predominantly $CH_3(v=0)$ formation regardless of the CH_4 vibrational mode. This result is in marked contrast to the quantum scattering calculation by Yu and Nyman,[13] where they predict a strong correlation between the CH_4 and CH_3 vibrations. Even though we observe an increase in $CH_3(\nu_2=1)$ population upon $\nu_2+\nu_4$ or ν_3 mode excitation of the CH_4, the fractional population of the $CH_3(\nu_2=1)$ products from the $Cl+CH_4(\nu_2+\nu_4)$ reaction is not greater than those from the $Cl+CH_4(\nu_3)$ reaction.

TABLE I. Intensity ratios of 2_1^1 and 0_0^0 bands of REMPI spectra of CH_3 products from the reactions $Cl+CH_4(\nu_2+\nu_4)$, $Cl+CH_4(\nu_3)$, and $Cl+CH_4(v=0)$.

	$Cl+CH_4(\nu_2+\nu_4)$	$Cl+CH_4(\nu_3)$	$Cl+CH_4(v=0)$
$\mathbf{I}(2_1^1)/\mathbf{I}(0_0^0)$	0.21 ± 0.04[a]	0.28 ± 0.06[a]	0.04[b]

[a]Uncertainties represent $2\sigma_{n-1}$ of replicate measurements.
[b]Upper bound.

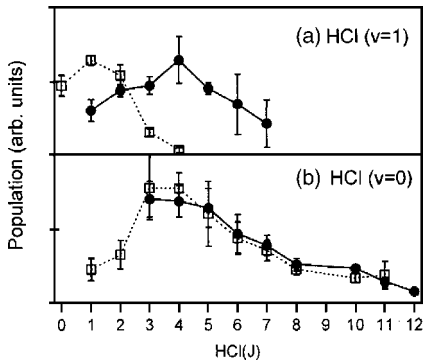

FIG. 5. (a) HCl($v=1$) and (b) HCl($v=0$) product rotational distributions from the $Cl+CH_4(\nu_2+\nu_4)$ (filled circles and solid lines) reaction. Also shown in open squares are the corresponding distributions from the $Cl+CH_4(\nu_3)$ reaction reproduced from Simpson *et al.* (Ref. 2). The error bars represent the $2\sigma_{n-1}$ of replicate measurements.

C. HCl product state distributions

Figure 5 displays the rotational distributions for the HCl($v=0$) and HCl($v=1$) products from the $Cl+CH_4(\nu_2+\nu_4)$ and $Cl+CH_4(\nu_3)$ reactions obtained by a method similar to that described by Simpson *et al.*[2] For the HCl($v=0$) distribution, population with $J<3$ cannot be recorded because of severe interference from the HCl($v=0$) background present in the expansion mixture. Consequently, the evaluation of the vibrational branching between the HCl ($v=0$) and HCl($v=1$) products is not possible. Overall, both HCl vibrational states exhibit cold distributions (rotational energy is less than a few percent of the total available energy), similar to other Cl+hydrocarbon (CH_4, C_2H_6, and C_3H_8) reactions studied so far. This cold distribution has been attributed to the kinematic constraints of the heavy-light-heavy reaction systems.[26]

The HCl ($v=0$) distributions from the $Cl+CH_4(\nu_2+\nu_4)$ and $Cl+CH_4(\nu_3)$ reactions are similar. On the other hand, the HCl ($v=1$) distributions are different for $\nu_2+\nu_4$ and ν_3 mode excitations: the distribution from $CH_4(\nu_2+\nu_4)$ peaks at $J=4$ and has average rotational energy of 228 cm^{-1}, whereas the distribution from $CH_4(\nu_3)$ peaks at $J=1$ and has only 41 cm^{-1} of average rotational energy. The difference in rotational distributions is surprising because the total energies of the two reactions are the same within 4%. Moreover, the total energy of the reaction with $CH_4(\nu_2+\nu_4)$ is *lower* than that of $CH_4(\nu_3)$. Our observation constitutes another example of *mode-specificity* in atom-polyatom reactions, where nearly

isoenergetic yet different vibrational excitations lead to markedly different rotational distributions of the products. Analogous mode-specific rotational distributions have been recently reported in the stretching mode mediated $Cl+CH_2D_2$ reaction.[3]

In stretch-mediated reactions such as $Cl+CH_4(\nu_3)$,[2] $Cl+CH_4(\nu_1)$,[6] or $Cl+CH_4(2\nu_3)$,[4] formation of vibrationally excited HCl products can be explained by a simple collinear vibrational energy transfer from C–H to H–Cl oscillators, based on the local oscillator picture of the C–H stretching vibration. On the other hand, the formation of $HCl(v=1)$ products from the $\nu_2+\nu_4$ mode mediated reaction is not likely to originate from a similar collinear vibrational energy transfer. Instead, we suggest that the formation of $HCl(v=1)$ product occurs through noncollinear vibrational energy transfer from the C–H bending motion to the HCl vibration. If we approximate the $\nu_2+\nu_4$ mode as the tangential motion of H atoms around the central C atom in methane, efficient transfer of the bending energy into the HCl bond can be achieved with a significantly bent Cl–H–C transition state. Therefore, $HCl(v=1)$ products are rotationally excited by the torque experienced during the separation stage of the HCl and CH_3 products. In contrast, a collinear geometry is favored for the formation of the $HCl(v=1)$ products from the $Cl+CH_4(\nu_3)$ reaction, and the rotational excitation of the HCl is small.

Enhanced rotational excitation of the product upon bending-mode excitation of the polyatomic reagents has been theoretically predicted for the $Cl+CH_4$,[15] $H+H_2O$,[11] and Cl+HOD (Ref. 10) reactions. In particular, Skokov and Bowman[15] recently carried out reduced dimensionality quantum scattering calculations on the $Cl+CH_4(2\nu_4)$ reaction and predicted a bimodal rotational distribution of HCl products, which is caused by a "mapping" of the Franck–Condon-type for the bending-mode wave function onto the rotational distribution of the HCl product.

D. Differential cross sections

Figure 6 shows the isotropic and anisotropic components of the core-extracted TOF profiles of $HCl(v=0,J=6)$ [Fig. 6(a)] and $HCl(v=0,J=10)$ [Fig. 6(b)] products from the $Cl+CH_4(\nu_2+\nu_4)$ reaction, and $HCl(v=0,J=5)$ [Fig. 6(c)] products from the $C+CH_4(\nu_3)$ reaction, obtained using the *R*-branch lines of the *F*-*X* (0,0) band. Poor signal-to-noise ratio prevented us from obtaining reliable TOF profiles of $HCl(v=1)$ products, and only the $HCl(v=0)$ products with $J>5$ have a sufficiently large signal-to-background ratio to permit us to obtain the TOF profiles of $HCl(v=0)$ products.

The isotropic component of the TOF profiles provides the laboratory-frame product distribution, whereas the ratio of the anisotropic and isotropic component for a given laboratory velocity determines the spatial anisotropies of the product. The spatial anisotropy $[\beta_{rxn}(v)]$ analysis of the state-selected $HCl(v=0)$ products (not shown) indicate that majority of the $HCl(v=0)$ products are formed in coincidence with $CH_3(v=0)$. Using this information, we convert the laboratory-frame speed distributions into the CM DCSs

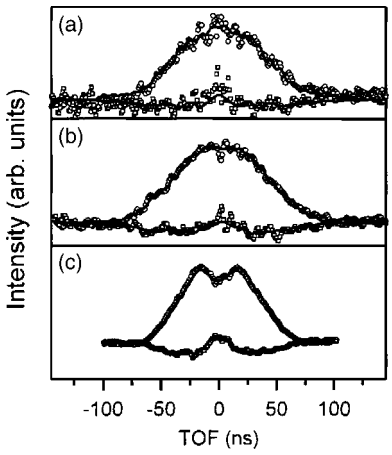

FIG. 6. The isotropic (open circles) and the anisotropic (open squares) components of the TOF profiles of (a) $HCl(v=0,J=6)$ and (b) $HCl(v=0,J=10)$ products from the $Cl+CH_4(\nu_2+\nu_4)$ reaction, and the TOF profile of (c) $HCl(v=0,J=5)$ product from the $Cl+CH_4(\nu_3)$ reaction. Also shown are the results of the fits (solid lines).

of the HCl $(v=0)$ products, which are shown in Fig. 7. The angular distributions of the HCl $(v=0,J=6)$ and HCl $(v=0,J=10)$ products from the $Cl+CH_4(\nu_2+\nu_4)$ reaction show broad side/backward scattering, and this broad backward scattering is consistent with the results of the quantum scattering calculation for the $Cl+CH_4(\nu_4)$ reaction by Yu and Nyman.[13]

The DCSs of the HCl $(v=0)$ product show a qualitatively similar trend (backward scattering) as the corresponding DCSs from the $Cl+CH_4(\nu_3)$ reaction. It is interesting to note that the nearly thermoneutral channel, HCl $(v=1)+CH_3(v=0)$, shows a dramatic mode specificity in the rotational distribution, whereas the exothermic product channel, $HCl(v=0)+CH_3$, exhibits no or only marginal specificity in the rotational distribution and the DCS. One explanation can be given in terms of the difference in geometric constraints

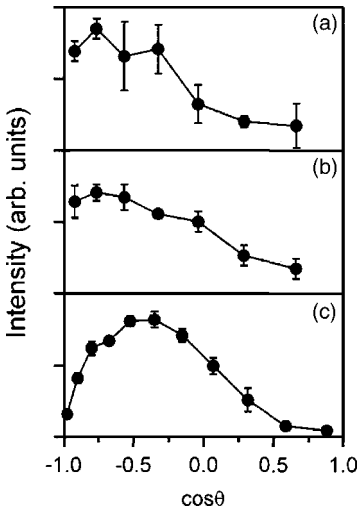

FIG. 7. DCSs for (a) $HCl(v=0,J=6)$ and (b) $HCl(v=0,J=10)$ from the $Cl+CH_4(\nu_2+\nu_4)$ reaction (circles and solid lines), and DCS of $HCl(v=0,J=5)$ product from the $Cl+CH_4(\nu_3)$ reaction. The error bars represent the $2\sigma_{n-1}$ of the replicate measurements.

associated with the product channels. For nearly thermoneutral channels [$HCl(v=1)$ product channels], geometries of the transition state are likely to be restricted. As mentioned above, the $Cl+CH_4(\nu_2+\nu_4)$ and $Cl+CH_4(\nu_3)$ reactions have different transition state geometries that lead to $HCl(v=1)$ product formation. Therefore, we expect that this difference in the transition state is reflected in the DCSs and rotational distributions. We also expect that these geometrical restrictions are significantly removed for the exothermic channels in the $CH_4(\nu_2+\nu_4)$ and $Cl+CH_4(\nu_3)$ reactions, which lead to mostly nonspecific behavior.

IV. SUMMARY AND CONCLUSIONS

In this work, we have compared the relative reactivities, product quantum state distributions, and differential cross sections of the $Cl+CH_4(\nu_2+\nu_4)$ and $Cl+CH_4(\nu_3)$ reactions. It is found that the $Cl+CH_4(\nu_2+\nu_4)$ reaction is at least 15% as reactive as the $Cl+CH_4(\nu_3)$ reaction. In strong contrast to theoretical predictions, we found no noticeable propensity for the formation of $CH_3(\nu_2=1)$ in the $Cl+CH_4(\nu_2+\nu_4)$ reaction. Instead, most of the CH_3 products are formed in the vibrational ground state. The $HCl(v=1)$ products from the $Cl+CH_4(\nu_2+\nu_4)$ reaction show an enhanced rotational excitation as compared with the corresponding products from the $Cl+CH_4(\nu_3)$ reaction. We propose that this rotational excitation can be explained in terms of the projection of the tangential motion of the C–H bond on to the rotational motion of the product. The differential cross sections of the $HCl(v=0)$ products show broad backward scattering behavior, which is in qualitative agreement with theoretical predictions on $Cl+CH_4(\nu_4)$ reaction. Our results clearly demonstrate that the bending vibration modes (ν_2 or ν_4) of methane play an active role in the reaction dynamics of atomic chlorine and methane.

ACKNOWLEDGMENTS

H.A.B. and J.P.C. thank the National Science Foundation for graduate fellowships. H.A.B. also acknowledges Stanford University for the award of a Stanford Graduate Fellowship. This work was supported by the National Science Foundation under Grant No. NSF-CHE-0242103.

[1] A. Sinha, M. C. Hsiao, and F. F. Crim, J. Chem. Phys. **94**, 4928 (1991); M. J. Bronikowski, W. R. Simpson, B. Girard, and R. N. Zare, *ibid.* **95**, 8647 (1991); M. J. Bronikowski, W. R. Simpson, and R. N. Zare, J. Phys. Chem. **97**, 2194 (1993); R. N. Zare, Science **279**, 1875 (1998); F. F. Crim, Acc. Chem. Res. **32**, 877 (1999); S. Yoon, R. J. Holiday, E. L. Sibert, and F. F. Crim, J. Chem. Phys. **119**, 9568 (2003); S. Yoon, R. J. Holiday, and F. F. Crim, *ibid.* **119**, 4755 (2003).
[2] W. R. Simpson, T. P. Rakitzis, S. A. Kandel, A. J. Orr-Ewing, and R. N. Zare, J. Chem. Phys. **103**, 7313 (1995).
[3] H. A. Bechtel, Z. H. Kim, J. P. Camden, and R. N. Zare, J. Chem. Phys. **120**, 791 (2004).
[4] Z. H. Kim, H. A. Bechtel, and R. N. Zare, J. Am. Chem. Soc. **123**, 12714 (2001); J. Chem. Phys. **117**, 3232 (2002).
[5] S. Yoon, S. Henton, A. N. Zivkovic, and F. F. Crim, J. Chem. Phys. **116**, 10744 (2002).
[6] H. A. Bechtel, J. P. Camden, and R. N. Zare, J. Chem. Phys. **120**, 5096 (2004).
[7] A. Sinha, J. D. Thoemke, and F. F. Crim, J. Chem. Phys. **96**, 372 (1992).
[8] E. Woods III, C. M. Cheatum, and F. F. Crim, J. Chem. Phys. **111**, 5829 (1999).
[9] M. J. Bronikowski, W. R. Simpson, and R. N. Zare, J. Phys. Chem. **97**, 2204 (1993).
[10] G. Nyman and D. C. Clary, J. Chem. Phys. **100**, 3556 (1994).
[11] D. Wang and J. M. Bowman, Chem. Phys. Lett. **207**, 227 (1993); D. C. Clary, J. Chem. Phys. **96**, 3656 (1992).
[12] J. C. Corchado, D. G. Truhlar, and J. Espinosa-Garcia, J. Chem. Phys. **112**, 9375 (2000).
[13] H.-G. Yu and G. Nyman, Phys. Chem. Chem. Phys. **1**, 1181 (1999).
[14] H.-G. Yu and G. Nyman, J. Chem. Phys. **110**, 7233 (1999).
[15] S. Skokov and J. M. Bowman, J. Chem. Phys. **113**, 4495 (2000).
[16] S. A. Kandel and R. N. Zare, J. Chem. Phys. **109**, 9719 (1998).
[17] A. R. Ravishankara and P. H. Wine, J. Chem. Phys. **72**, 25 (1980); H. A. Michelsen, Acc. Chem. Res. **34**, 331 (2001).
[18] J. Zhou, J. J. Lin, B. Zhang, and K. Liu, J. Phys. Chem. A **108**, 7832 (2004).
[19] R. Atkinson, D. L. Baulch, R. A. Cox, R. F. Hampton, Jr., J. A. Kerr, and J. Troe, J. Phys. Chem. Ref. Data **21**, 1125 (1992).
[20] P. C. Samartzis, B. Bakker, T. P. Rakitzis, D. H. Parker, and T. N. Kitsopoulos, J. Chem. Phys. **110**, 5201 (1999).
[21] L. S. Rothman, *HITRAN 2000 Spectral Database* (HITRAN, Cambridge, 2000).
[22] L. R. Brown, R. A. Toth, A. G. Robiette, J. E. Lolck, R. H. Hunt, and J. W. Brault, J. Mol. Spectrosc. **93**, 317 (1982).
[23] J. W. Hudgens, T. G. DiGiuseppe, and M. C. Lin, J. Chem. Phys. **79**, 571 (1983).
[24] W. Demtröder, *Laser Spectroscopy*, 2nd ed. (Springer, New York, 1995), pp. 92–95.
[25] E. Venuti, L. Halonen, and R. G. D. Valle, J. Chem. Phys. **110**, 7339 (1999).
[26] C. A. Picconatto, A. Srivastava, and J. J. Valentini, J. Chem. Phys. **114**, 1163 (2001).
[27] W. J. van der Zande, R. Zhang, R. N. Zare, K. G. McKendrick, and J. J. Valentini, J. Phys. Chem. **95**, 8205 (1991).